



A transient model for the thermal inertia of chilled-water systems during demand response



Weilin Li^a, Yiyi Chu^a, Peng Xu^{a,*}, Zhiwei Yang^a, Ying Ji^a, Lizhou Ni^b, Yi Bao^b, Kun Wang^b

^a College of Mechanical and Power Engineering, Tongji University, Cao'an Road No. 4800, Shanghai, 201804, China

^b Hangzhou Telek Technology Co., Wenhui Road No.303, Hangzhou, 310014, China

ARTICLE INFO

Article history:

Received 11 November 2016

Received in revised form 25 April 2017

Accepted 30 May 2017

Available online 7 June 2017

Keywords:

Demand response (DR)

Thermal inertia model

Transient air-conditioning model

Chilled-water system

ABSTRACT

Demand response (DR) of air-conditioning systems is important to shift or reduce the peak electricity demand of commercial buildings by shift or reduce the cooling load. Popular DR strategies of air-conditioning systems include zonal temperature reset and direct control of the main equipment. Many DR studies have been conducted on the thermal inertia of buildings for temperature resetting, but there are few studies on the thermal inertia of air-conditioning systems, which is relatively small but not negligible. In this paper, the thermal inertia of air-conditioning systems is defined as the character that causes the variation of the supply cooling capacity to zones lagging behind the variation of the cooling capacity from plants after DR strategies are implemented. This paper develops an inertia model of chilled-water systems with three sub-models, including chiller model, chilled-water pipe model and cooling coil model. The model describes the dynamic process from the cooling plant to terminal units when DR strategies on chillers are implemented. A new parameter $Q(t)$ named the “refrigerant cooling capacity” is introduced in this study to simplify the thermal inertia model. The $Q(t)$ patterns during the dynamic processes of two series of common chiller-side control strategies (On/Off control and resetting the chilled-water temperature) are obtained and validated using experiments and field tests. In the end, the entire transient model of air-conditioning systems is validated using experiments.

© 2017 Elsevier B.V. All rights reserved.

1. Introduction

Global building energy consumption has steadily increased [1]. The building sector represents over 40% of worldwide primary energy consumption [2]. The growth in energy use for heating, ventilation and air conditioning (HVAC) systems is particularly significant [3]. The energy consumed by electric air-conditioning is 30–50% of the total electric energy consumed during summer in many cities worldwide. This proportion even exceeds 50% in some commercially dense and developed cities [4]. In addition to the accumulated energy use, buildings, particularly commercial buildings, tend to simultaneously have high electricity demand under heat waves, which causes significant peak demand exertion on the grid [5]. Particularly, in extreme weather, the peak load caused by air-conditioning systems can jeopardize the grid. Recently, the demand response (DR), which is a technology that is used to flatten the peak, has become a popular solution in both the US and European electricity markets [6,7]. The DR can be defined as “changes in

electric usage by end-use customers from their normal consumption patterns in response to changes in the price of electricity over time, or to incentive payments designed to induce lower electricity use at times of high wholesale market prices or when system reliability is jeopardized.” [8]

Feasible DR strategies for heating, ventilation and air-conditioning (HVAC) systems were summarized by Motegi et al. [9]. The literature indicates that HVAC-based DR strategies for a given facility are subjected to the type and condition of the building, mechanical equipment, and energy management and control systems (EMCS). Three commonly used DR strategies focus on different parts of the building and systems. They include zone temperature control, air distribution control, central-plant control strategies, and so on. Among these strategies, many researchers [10–18] have focused on the study of zone control strategies, i.e., temperature adjustment and passive thermal mass storage. In 2002, Braun et al. [10] conducted a simple temperature reset control strategy to validate the feasibility of using the thermal inertia of a building to shift the peak load of the air-conditioning system. Xu [12] studied the potential of pre-cooling and demand limiting by adjusting the zone temperature set points in heavy-mass and light-mass buildings of California and demonstrated that the strategy significantly

* Corresponding author.

E-mail address: xupengwb@gmail.com (P. Xu).

Nomenclature

A	Heat transfer area, m^2
c	Specific heat, $J/(kg \cdot ^\circ C)$
h	Enthalpy, J/kg
m	Total mass, kg
NTU	Number of heat transfer unit
n_x	Constant
R	Heat resistant, $^\circ C/W$
T	Temperature, $^\circ C$
α	Coefficient of convection heat transfer, $W/(m^2 \cdot ^\circ C)$
α'	Coefficient of convection heat transfer under dehumidification, $W/(m^2 \cdot ^\circ C)$
ε	Heat transfer effectiveness
η	the overall fin efficiency for heat transfer only
η'	the overall fin efficiency for both air-side heat and mass transfer
λ	Thermal conductivity, $W/(m^2 \cdot ^\circ C)$
C_x	Constant
d	Hydraulic diameter, m
\dot{M}	Mass flow rate, kg/s
N	Arbitrary number of control volumes for coil
Nu	Nusselt number
Q	Cooling capacity, W
Re	Reynolds number
t	Time, s
<i>Superscript</i>	
ch	Chiller
co	Coil
pi	Pipe
<i>Subscript</i>	
a	Air
c	Coil material
e	Evaporator material
in	Inlet
ins	Insulation material
out	Outlet
p	Pipe
r	Refrigerant
s	Saturation
tot	Total
w	Water

reduced the cooling load in both light- and heavy-mass buildings. Lee and Braun [14–16] developed a simple approach to estimate the building zone temperature setpoint variations to minimize the peak cooling demands.

However, the EMCS is required to support the global reset of zone temperatures to implement demand-shifting strategies based on zone temperature reset. Therefore, temperature adjustment is not a universal strategy. When EMCS does not support the global reset of zone temperatures, central-plant control strategies can be used, such as resetting the supply chilled-water temperature or shutting down some chillers [13]. The DR controls in previous temperature adjustment studies have inherent and significant delays [19]. Xue et al. [19] proposed a fast DR control strategy for commercial buildings from the chiller plant side. Keeney and Braun [20] developed and tested a control strategy for an office building to limit the peak cooling load and continue building operation if one of the four central chiller units was shut down. Through a survey of large commercial buildings, Song et al. [21] noted that most occupants did not feel the interruption of the cooling supply when

the air-conditioning system shut down for 10–20 min per hour. It is observed that central-plant control strategies can effectively shift or reduce the peak load of air-conditioning systems.

An air-conditioning system can shift or reduce the peak cooling load without affecting the thermal comfort of occupants by using the thermal inertia of the building [22]. Most studies focused on developing an accuracy model of the building thermal inertia while simplified or ignored the dynamic character and thermal inertia of the air-conditioning system. However, plant-side control strategies, such as shut off the chillers, and increase the chilled-water temperature, which also take advantage of the thermal inertia character of the air-conditioning system. This inertia delays the temperature increase of the chilled water and keeps supplying cooling to zones. In this study, this character is called the “thermal inertia of air-conditioning system”, which is defined as the character that causes the variation of the supply cooling capacity to zones lagging behind the variation of the cooling capacity from plants.

Different from the existing studies on DR of the air conditioning system, this paper focuses more on the control strategies of the chiller side, concerning the thermal inertia of the air conditioning system during DR events. This study is intended to provide a thermal inertia model of the air conditioning system, combining the theoretical and experimental methods, so as to predict the dynamic variation of the cooling capacity after DR control strategies are implemented.

This paper is organized as follows: Section 2 reviews the related literatures about dynamic model air-conditioning systems, and reviews the models of the chilled water side in detail, including chiller, cooling coil and chilled-water pipe; section 3 develops the thermal inertia model of the air-conditioning system; and section 4 validates the models using experiments. Discussions and conclusions are provided in sections 5.

2. Dynamic air-conditioning system model review

Dynamic models of air-conditioning systems can be valuable tools to predict system behavior during the start-up, feedback control and shutdown [23].

Pengfei Li et al. [24,25] have reviewed the previous work on HVAC equipment modeling comprehensively, including vapor compression cycles, air-handling units, major types of chillers, cooling tower, heating systems, and renewable-energy driven systems. Shengwei Wang [26] presented a traditional component-based dynamic model to simulate the thermal, hydraulic, environmental and mechanic characteristics and energy performance of a building and VAV air-conditioning system. Chen Wu et al. [27] developed a simplified lumped parameter dynamic model for a triple evaporator air conditioner. Bourhan Tashtoush et al. [28] described a dynamic model of an HVAC system including a zone, heating coil, cooling and dehumidifying coil, humidifier, ductwork, fan, and mixing box. Mossolly et al. [29] presented a space and equipment mathematical model consisting of models for air handling unit of the HVAC system to predict energy consumption of various components in response to optimized set points of the selected control strategy. Glenn Platt [30] developed a mathematical model of the HVAC system based on physical principles and circuit theory.

The dynamic models appeared in the above literature are formulated from physical fundamentals such as mass continuity, energy conservation and heat transfer laws by using a lumped-parameter model and physical relations, which are called physical-based models or white-box models [31].

The data-based strategy or black-box model, based on mathematical rules to obtain the formulation of the system from experimental data, is also used in the dynamic model of the air conditioning systems [32–34]. Although the performance param-

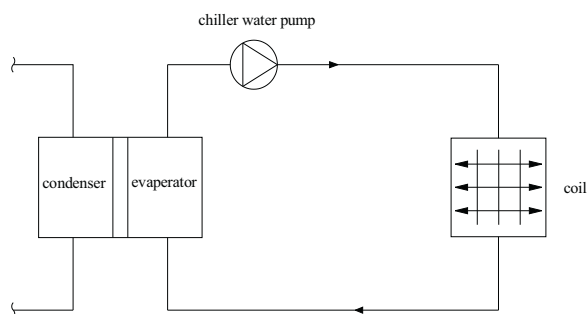


Fig. 1. Sketch of a commercial air-conditioning system.

eters of these systems can easily be determined by mathematical model using statistical methods, however they are fully empirical and difficult to be generalized, and perfect training data sets are needed to ensure the accuracy of the data-based model under different dynamic conditions [35]. DR strategies are different from common strategies, for DR strategies will be enforced only when DR events occur. Thus, the dynamic operating data during DR periods is difficult to be attained before DR happens to train the data-based model.

The first-principle models could reveal the dynamic relationship between the system and various disturbances which are all taken into consideration to make better control strategies [36]. This paper aims at exploring the heat transfer principle to predict the dynamic variation of the cooling capacity after DR control strategies implemented. Therefore, a physical-based dynamic model of chilled water systems in commercial buildings to describe the thermal inertia of air-conditioning systems was developed in this paper.

In DR study, the dynamic model of air-conditioning systems becomes particularly important. It is largely because DR control strategies use the thermal inertia of the air conditioning system to slash the power of the air conditioning in a short time and maintain the cooling supply at the same time. As mentioned before, the paper focused on the thermal inertia of chilled-water systems and aims to describe supply cooling capacity to zones, which can be used to predict the indoor temperature during DR. Therefore, the researches of the physical-based model of chilled water side are reviewed further.

A typical chilled water system of commercial air-conditioning is shown in Fig. 1. The thermal inertia substance includes the water, refrigerant and material of each device. Therefore, the major components that have thermal inertia are the chillers, transmission and distribution pipes, and cooling coils.

2.1. Dynamic chiller model review

The most difficult part of building a dynamic model of chillers is to find a simple and accurate dynamic heat exchanger (evaporator and condenser) model. Wedekind et al. [37] studied the transient behavior of two-phase flow dynamics in heat exchangers and noted that the complete two-phase region could be treated in adequate detail even in a lumped form. Deng [38] presented a dynamic model of a direct expansion water-cooled air-conditioning plant, including a compressor, a thermostatic expansion valve, a water cooled condenser and a direct expansion evaporator. Rasmussen et al. [39] developed a different modeling approach, the energy based approach using lumped parameter approach, shows obvious freedom in choosing the state variables and is more straightforward to derive and simpler conceptually for a transcritical vapor compression system. Browne and Bansal [40] presented a transient simulation model to predict the dynamic performance of vapor compression liquid chillers under different operating conditions. The model uses a thermal capacitance approach for specific

state variables to account for the dynamics of the exchangers and ancillaries. The model is relatively simple and requires only few initial conditions. Zhao and Zaheeruddin [41] developed a lumped-parameter dynamic model of a water chiller refrigeration system based on mass and energy balance principles. The transient response characteristics show that the thermal system responses are much slower than the pressure and mass flow rate responses, which reveal a two time-scale property of the system. Llopis et al. [42] presents a mathematical model of a shell-and-tube condenser based on the mass continuity, energy conservation and heat transfer physical fundamentals, whose methodology can be easily adapted to model any type of condenser. Yao et al. [36] developed a state-space model to investigate the dynamic behaviors of refrigeration systems. Ordinary differential equations that describe the chiller's dynamic thermal behaviors are transformed into a representation form of the state space, using the vector-matrix notation and linearization. Nunes et al. [43] introduced a dimensionless simplified mathematical model of a vapor compression refrigeration system to optimize the system dynamic response.

In our study, we develop a dynamic chiller model based on the integration of mass, energy and momentum balance. A new parameter, which is the refrigerant cooling capacity $Q(t)$, is introduced to simplify the modeling process, as shown in section 3.

2.2. Dynamic cooling coil model review

Cooling-coil models have been studied for many years and are commonly divided into steady-state and dynamic models [44]. This paper focuses on developing a dynamic model to describe the thermal inertia of an HVAC system during DR. Therefore, only dynamic models of cooling coils are reviewed.

Yu et al. [44] developed models for the dynamic performance of dry and wet cooling coils. They established a dry-area model without consideration of condensation with three energy equations and a wet-area model based on a mass balance equation for moist air as well as three energy equations for the air, tube/fin, and working fluid. Lee [45] proposed a simplified explicit model for the chilled-water cooling coil, which could determine the performance of a partially wet coil without requiring iterative calculations.

These coil models can well describe the dynamic performance of cooling coils. However, many parameters, such as the parameters of the coil construction, working fluid, tube and fin, are required to establish the models, which are difficult to obtain.

Jin et al. [46] developed a dynamic cooling-coil unit model by extending the cooling-coil unit engineering model and combining the model with the mass and energy balance equations. Six model parameters of the model were estimated using commissioning information with a nonlinear online identification method. Unlike the aforementioned dynamic models, this model obtained the nonlinear characteristics over a wide operating range of the cooling-coil unit without requiring the geometric and physical parameters.

Zhou and Braun [47] developed a distributed model for the transient behavior of cooling and dehumidifying coils, which used several steady-state performance indices to simplify the dynamic modeling. The model was validated to accurately predict the coil transient performance for four- and eight-row coils by comparisons with detailed experimental measurements [48].

The doctoral thesis of Zhou [49] detailed the process of simplification and verified the reasonability of these simplifications. For example, the effect of the heat capacitance of water condensate could be considered to be negligible, and a model based on a pure counter-flow arrangement was used to simplify the counter cross-flow model.

The detailed model of cooling coils was simplified by Zhou [49], and the necessary coefficients of the model equations were obtained using the operational parameters of a short period to

avoid a detailed description of coil. In this study, the coil model refers to the model that Zhou developed. The model is trained using operational parameters of the cooling coil in this study.

2.3. Dynamic water pipe model review

The thermal inertia of transmission and distribution pipes and the chilled water in the pipes are non-negligible. In the building energy simulation software EnergyPlus [50] and energy system simulation software TRNSYS [51], the models of the chiller and coil do not describe the thermal inertia of the materials and the coolant. However, the pipe models of the software are dynamic models that consider the heat capacity of the pipe material and chilled water.

The dynamic simulation of the duct and pipe behavior has been studied less intensively than that of most HVAC components [52]. Hanby et al. [52] developed a method to dynamically model a fluid conduit based on discretization into a sequence of well mixed flow nodes, which could calculate the response to changes in the flow rate and fluid inlet temperature.

In our study, we develop the thermal inertia model of the pipe based on the dynamic heat transfer principles.

3. Dynamic air-conditioning system model

The main difference of the proposed model in this study is the emphasis of the thermal inertia, whereas previous studies focused on the overall performance of air-conditioning systems, which are more complicated and not focus on DR strategies. In the DR event, the accurate modeling of the air-conditioning system is as important as the behavior of the 15–30 min after the plant is shut off or reset. Therefore, in this study, a detailed model of every device is unnecessary, while the model must accurately describe the change of the chilled-water temperature and supply air temperature during the DR period. The accurate prediction of the change is pivotal to maintain the indoor temperature in the comfort zone when DR occurs.

The characters of the proposed model are as follows:

- The chiller model should be able to describe the change in the chilled-water temperature after DR control strategies are implemented;
- The cooling-coil model should be able to describe the change in the supply air temperature;
- The pipe model should be able to calculate the temperature of the outlet water when the temperature of the inlet water changes.

3.1. Chiller model

Some universal assumptions and simplifications are adopted before chiller modeling to avoid some unnecessary complication [23,36,37,40,41,53].

- The temperature of the chilled water is reset by compressor unloading. Comparing to the thermal delay, the delay of the compressor adjustment is negligible;
- The flow rate of the refrigerant during the entire circle is constant, and the refrigerant masses in the evaporator and condenser are constant;
- The relative flow between the water (coolant) and refrigerant is simplified as a pure counter flow;
- The temperature variation of the chilled water is linear along the evaporator, and the shell temperature is described as an average value;
- The dynamic storage of the mass and energy in the superheated vapor region is negligible.

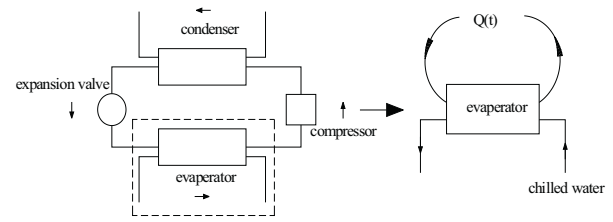


Fig. 2. Simplification of the chilled thermal inertia model.

- The two-phase flow can be represented by a single-phase flow with average properties.

Based on these assumptions, the emphasis of the dynamic model of the chiller is to describe the cooling capacity variation of chilled water when DR strategies happened. The detailed descriptions of compressor, condenser, and expansion valve are unnecessary for this purpose. Therefore, the boundary conditions of the chiller model are moved inward and a new parameter, called “refrigerant cooling capacity”, is introduced to describe the influence of compressor, condenser, and expansion valve on the refrigerant cooling capacity of evaporator (Fig. 2). Thus, the chiller model is simplified to a considerable degree and is not restricted by the form of the cooling side. The simplified dynamic model of the chiller is developed according to the principle of energy conservation.

3.1.1. Equations

The common DR control strategies used in cooling plants include shutting down chillers, intermittently cycling chillers, shutting down the chiller while maintaining the pump operation, and increasing the chilled-water setpoint. These control strategies reduce the electricity demand of the air-conditioning system by unloading chillers. Thus, the cooling capacity generated by the plant reduces from $Q(t)_{t=0}$ to $Q(t)$ until it reaches a new steady state.

The dynamic heat balance equation of the refrigerant is:

$$c_r m_r \frac{dT_r}{dt} = Q(t) + \alpha_{r-e} A_{r-e} (T_e - T_r) \quad (1)$$

The dynamic heat balance relationship of the evaporator is:

$$c_e m_e \frac{dT_e}{dt} = \alpha_{w-e} A_{w-e} \left(\frac{T_{w,in}^{ch} + T_{w,out}^{ch}}{2} - T_e \right) + \alpha_{r-e} A_{r-e} (T_r - T_e) \quad (2)$$

The dynamic heat balance of chilled water is:

$$c_w m_w \frac{dT_w}{dt} = \alpha_{w-e} A_{w-e} \left(T_e - \frac{T_{w,in}^{ch} + T_{w,out}^{ch}}{2} \right) + c_w \dot{M}_w (T_{w,in}^{ch} - T_{w,out}^{ch}) \quad (3)$$

Eqs. (1)–(3) are the transient model of chillers, which describes the dynamic process of the chiller to a new steady state after DR strategies are implemented.

3.1.2. Parameter specification

3.1.2.1. Displaced cooling capacity $Q(t)$. In the dynamic model of chillers, $Q(t)$ is the “refrigerant cooling capacity”, which presents the cooling capacity transferred to the refrigerant of the evaporator (Eq. (1) and Figure). Thus, the detailed dynamic variations of the compressor, condenser and expansion valve are replaced by a single variable, and the chiller dynamic model is significantly simplified.

3.1.2.2. *Steady stage.* In the steady stage, before the DR strategy is implemented or a new steady state is reached, all of dT_r/dt , dT_e/dt , and dT_w/dt are equal to 0. The cooling capacity of the chiller can be expressed as:

$$Q(t)_{t=0} = c_w \dot{M}_w (T_{w,in}^{ch} - T_{w,out}^{ch}) \quad (4)$$

In practical buildings, the temperatures of the return and supply chilled water $T_{w,in}^{ch}$ and $T_{w,out}^{ch}$ and the flow rate of chilled water \dot{M}_w are easily available parameters, which can be measured from temperature sensors and flow meters. Thus, the cooling capacity of the steady state is calculated using Eq. (4).

3.1.2.3. *Dynamic stage.* During the dynamic stage after the DR strategy is implemented, $Q(t)$ denotes the refrigerant cooling capacity of the dynamic process. Under the DR strategy of temporarily shutting down the chiller, $Q(t)$ is surmised to be zero. The variation pattern of $Q(t)$ is difficult to confirm by experience for resetting the temperature setpoint of chilled water. In this paper, $Q(t)$ of different DR control strategies were obtained and validated using experiments.

3.1.2.4. *Heat transfer coefficient α_{r-e} and α_{w-e} .* The heat transfer coefficient between the refrigerant and evaporator α_{r-e} and the heat transfer coefficient between water and the evaporator α_{w-e} are empirically calculated [36]:

$$\alpha_{r-e} = C_1 (T_e - T_r)^{n_1} \quad (5)$$

$$Nu_{w-e} = C_2 Re_w^{n_2} \quad (6)$$

$$\alpha_{w-e} = Nu_{w-e} \cdot \lambda_w / d_e \quad (7)$$

3.2. Coil model

An accurate and computationally fast coil model developed by Zhou [47–49] is used in this paper to described the thermal internal of the cooling coil. The important assumptions and simplifications in the model development are as follows:

- The energy stored in air is negligible;
- When dehumidification occurs, the effect of the water condensate on the fin and tube is negligible;
- The temperature profile in the fins in the fin-height direction follows the steady-state profile, which enables the use of heat transfer and combined heat and mass transfer fin efficiencies;
- A simplified model based on a pure counter-flow arrangement is used to avoid a detailed description of coil circuiting.

3.2.1. Equations

In this simplified model, for each discrete time interval, each row of the coil is treated as either all wet or all dry.

3.2.1.1. *Dry row.* The energy balance equation of the chilled water in the coil is:

$$c_w m_w \frac{dT_w^{co}}{dt} = c_w \dot{M}_w (T_{w,in}^{co} - T_{w,out}^{co}) + \frac{1}{R_w} \left(T_c - \frac{T_{w,in}^{co} + T_{w,out}^{co}}{2} \right) \quad (8)$$

The energy balance equation of the coil materials is:

$$c_c m_c \frac{dT_c}{dt} = \frac{1}{R_a} (T_{a,in} - T_c) + \frac{1}{R_w} \left(\frac{T_{w,in}^{co} + T_{w,out}^{co}}{2} - T_c \right) \quad (9)$$

3.2.1.2. *Wet row.* For a wet row, the energy balance equation of the coil materials, i.e., Eq. (9), is replaced by Eq. (10):

$$c_c m_c \frac{dT_c}{dt} = \frac{1}{R_a} (h_{a,in} - h_{s,c}) + \frac{1}{R_w} \left(\frac{T_{w,in}^{co} + T_{w,out}^{co}}{2} - T_c \right) \quad (10)$$

where $h_{s,c}$ is the saturation air enthalpy at the mean coil temperature T_c .

3.2.2. Parameter specification

3.2.2.1. *Water-side heat resistance for each row R_w .* In the simplified model, a pure counter-flow arrangement R_w can be calculated by:

$$R_w = \frac{N}{\alpha_{w-c} A_{w-c,tot}} \quad (11)$$

where $A_{w-c,tot}$ is the water-side total surface area of heat transfer.

3.2.2.2. *Air-side heat resistance for each row R_a .*

$$R_a = \frac{1}{\varepsilon_a c_a \dot{M}_a} \quad (12)$$

where ε_a is the water-side heat transfer effectiveness for the row, which can be calculated by:

$$\varepsilon_a = 1 - e^{-NTU_a} \quad (12)$$

$$NTU_a = \frac{\eta_a \alpha_{a-c} A_{a-c,tot}}{c_a \dot{M}_a N} \quad (13)$$

3.2.2.3. *Air-side total resistance for heat and mass transfer between the coil material and air R'_a .*

$$R'_a = \frac{1}{\varepsilon'_a \dot{M}_a} \quad (14)$$

where ε'_a is the air-side heat and mass transfer effectiveness, which can be calculated by:

$$\varepsilon'_a = 1 - e^{-NTU'_a} \quad (15)$$

$$\text{and } NTU'_a = \frac{\eta'_a \alpha'_{a-c} A_{a-c,tot}}{c_a \dot{M}_a N} \quad (16)$$

3.2.2.4. *Basic parameters.* Three groups of parameters must be confirmed for further calculation, $\alpha_{w-c} A_{w-c}$, $\eta_a \alpha_{a-c} A_{a-c,tot}$ and $\eta'_a \alpha'_{a-c} A_{a-c,tot}$. The empirical equations used to calculate these parameters are [47]:

$$\alpha_{w-c} A_{w-c,tot} = C_3 (\dot{M}_w)^{n_3} \quad (17)$$

$$\eta_a \alpha_{a-c} A_{a-c,tot} = C_4 (\dot{M}_a)^{n_4} \quad (18)$$

$$\eta'_a \alpha'_{a-c} A_{a-c,tot} = C_5 (\dot{M}_a)^{n_5} \quad (19)$$

where $C_5 = C_4 n_5 = n_4$, C_3 , C_4 , C_5 and n_3 , n_4 , n_5 , are determined by the regression of the coil operation data, which can be obtained using a short-term measurement.

3.3. Pipe model

The pipe dynamic model is developed according to the heat transfer principle and energy conversion. The pipe consists of three parts: the chilled water, pipe material and insulation material. Although the specific heat of the insulation material is high, its density (about 65 kg/m³) is two orders of magnitude less than that of the chilled water and pipe material. Therefore, in the model, the total heat capacity of the insulation material is assumed to be negligible. The insulation around the pipe is modeled as a steady state.

The pipe heat transfer is simulated by discretizing the pipe length into several nodes. The control volumes are shown in Fig. 3.

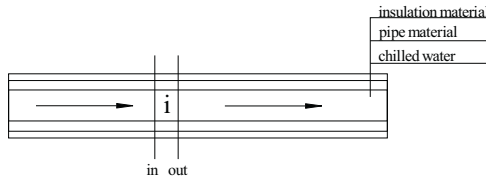


Fig. 3. Control volume drawn around node i .

3.3.1. Equations

The energy balance equation of the chilled water in control volume i is:

$$m_w c_w \frac{dT_w^{pi}}{dt} = c_w \dot{M}_w (T_{w,in}^{pi} - T_{w,out}^{pi}) + \alpha_{w-p} A_{w-p} \left(T_p - \frac{T_{w,in}^{pi} + T_{w,out}^{pi}}{2} \right) \quad (20)$$

The energy balance equation of the pipe material is:

$$m_p c_p \frac{dT_p}{dt} = \alpha_{w-p} A_{w-p} \left(\frac{T_{w,in}^{pi} + T_{w,out}^{pi}}{2} - T_p \right) + \alpha_{a-ins} A_{a-ins} (T_a - T_{ins}) \quad (21)$$

3.3.2. Parameter specification

The heat transfer coefficient between water and pipe α_{w-p} and the heat transfer coefficient between the insulation material and ambient air are determined as follows [53]:

$$Nu_{w-p} = C_6 Re_w^{n_6} Pr_f^{n_7} \quad (22)$$

$$Nu_{a-ins} = C_7 (Gr \cdot Pr)^{n_8} \quad (23)$$

$$\alpha_{w-p} = Nu_{w-p} \cdot \lambda_w / d_p \quad (24)$$

$$\alpha_{a-ins} = Nu_{a-ins} \cdot \lambda_a / d_{ins} \quad (25)$$

where C_6 , C_7 , and n_6 , n_7 , n_8 are constants, and the values under different situations are recommended in [53].

4. Experimental study

The entire thermal inertia model of the chilled-water system consists of the chiller model (1)–(3), cooling-coil model (8)–(10) and pipe model (20)–(21). The chiller model only considers the dynamic property of the evaporator and attributes all effects to the variation of $Q(t)$ which considerably simplifies the model. Therefore, during the model validation process, the first step is to verify the patterns of the $Q(t)$ of different DR control strategies. Then, new experiments were used to validate the $Q(t)$ and entire thermal inertia model. Finally, $Q(t)$ of different DR control strategies were further validated using a commercial chiller of a practical building. In summary, the validation process consists of three steps:

- Discretize and calculate the differential Eq. (1)–(3), (8)–(10) and (20), (21);
- Experimentally collect the operational parameters of different DR strategies;
- Collect the operational parameters of the commercial chiller under different DR strategies.

The detailed model validation process is shown in Fig. 4.

4.1. Control strategies selected

As mentioned in section 1, current researches on DR control strategies of the air conditioning system mostly focused on terminal control, requiring the support of the EMCS system [9,13]. On the one hand, most of EMCS system of existing commercial buildings cannot realize this kind of control such as global temperature reset in China, and on the other hand, traditional terminal DR strategies would be some response delay presented by scholars [19]. So the established model in this paper is concentrated on the chiller side strategies.

Motegi et al. [9] summarized the common strategies for chiller side, which are not too many and make it possible to attain the system operation variations of different DR strategies by experiments. The chiller side strategies consist of “chilled water temperature increase”, “chiller quantity Reduction” and “cycling the chillers”. According to American commercial building investigation [9], the “chilled water temperature increase” control strategy is highest frequently used, and except the strategies mentioned above others are seldom used.

The three control strategies mentioned above can further be divided into two types:

- On/Off control: Shut off chillers (part or all) while keeping chilled water pumps and terminals running to maintain the cooling supply to building and to decrease energy consumption of the chillers, which includes “Chiller quantity Reduction” and “cycling the chillers”.
- Chilled water temperature control: Increase chilled water temperature to improve chiller efficiency and reduce cooling load.

Therefore, two series of DR strategies were tested in this paper: shutting down the chiller (while maintaining the chilled water pump and the terminal operation) and increasing chilled water temperature.

4.2. Test validation

4.2.1. Experimental setup

The experimental platform is the HVAC system of the “Building Energy Efficiency Laboratory” in Shanghai, China.

The whole test platform is composed of two identical room and an environment control chamber (Fig. 5 (a)). The chamber and the rooms are equipped with two independent air conditioning systems to control the air temperature inside and outside the rooms. During the experiment, turning on the air conditioning system of the chamber could keep the external environment outside the room stable, namely constant external disturbance. The two rooms are vacant without internal disturbance, which ensures the stable operation of the air conditioning system before the strategies implemented.

During the experiment, only the terminal of one room is turned on and the other keeps closed. The schematic diagram of the system and placements of temperature sensors are shown in Fig. 5(b). The list and detailed information of all of the sensors in the experiments is shown in Table 1. Detailed information of these devices is shown in Table 2. The chiller is an air-cooled heat pump. The type of heat extraction side does not affect the model, for the thermal inertia model of the chiller in this paper only considers the thermal inertia of the chilled-water side. The temperature of the return chilled water can be reset using the control panel of the HVAC system. The terminal of the HVAC system is a fan-coil unit (FCU), and the air velocity of the FCU has three levels: High (680 m³/h), Medium (510 m³/h) and Low (357 m³/h). The fan running at 510 m³/h during the experiment.

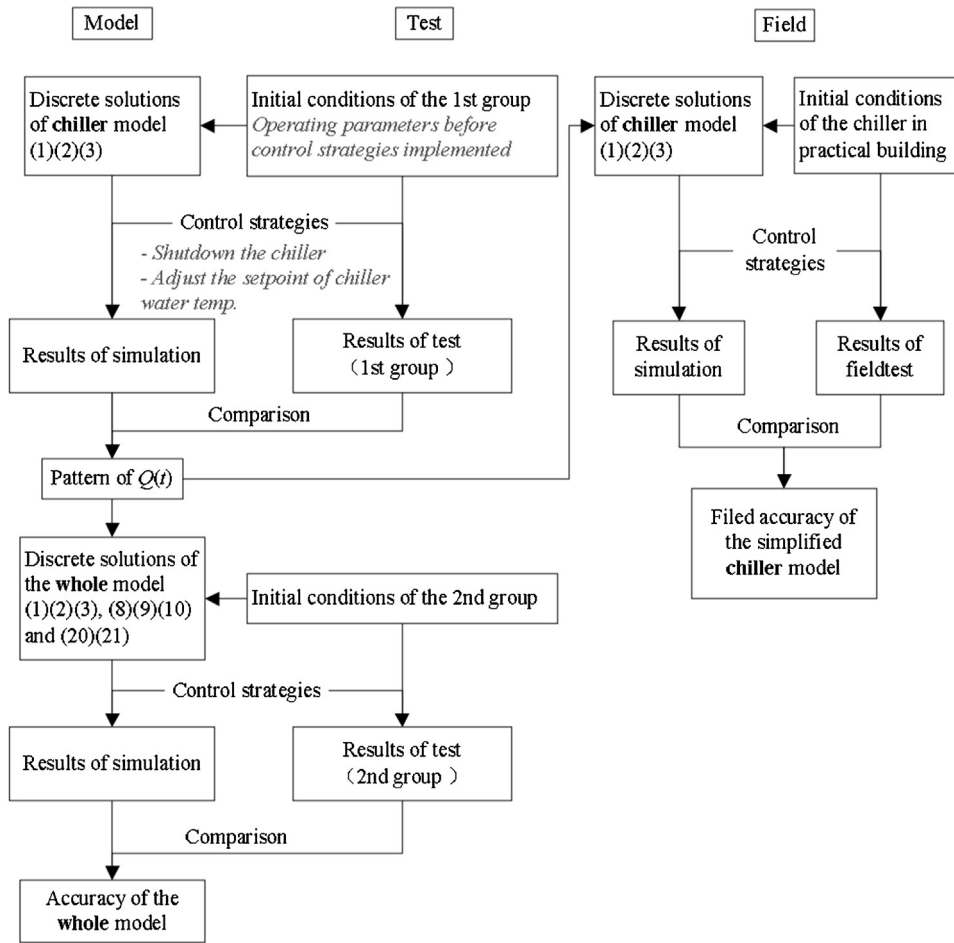


Fig. 4. Flow chart of the model validation.

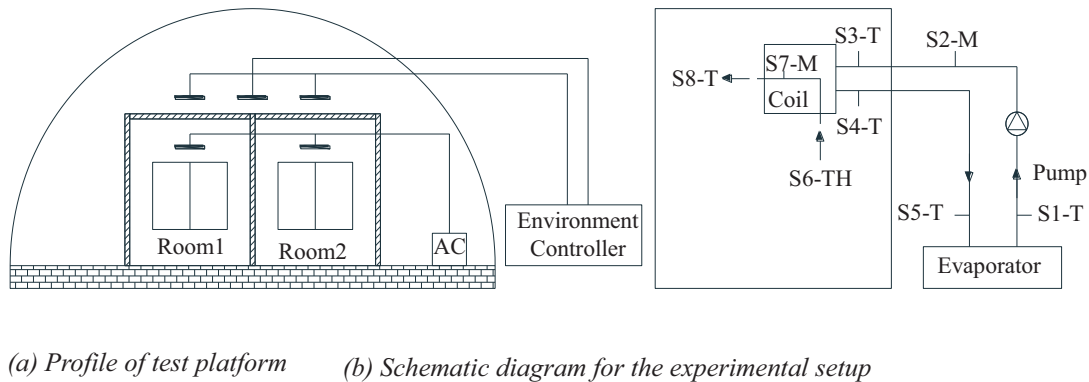


Fig. 5. Test platform.

The required sensors for the model calibration of the chiller, pipes and coil are shown in Table 2. Due to the experimental limitations, the measurement accuracy of the sensor S5-T measuring the return chilled water temperature is a little larger. S5-T is one of the necessary sensors for chiller model validation, so the accuracy of the sensor may produce error for solving $Q(t)$ and verifying the chiller model. Therefore, the chiller model and $Q(t)$ under different control strategies are validated again through an actual chiller in a commercial building. In addition, the calibration of the whole chilled water system can also illustrate the precision of the chiller model.

The values of the constant parameters C_x and n_x of this HVAC system are obtained using the regression method of the operation parameters under different steady states or the recommended parameters from [54], as shown in Table 3.

As mentioned above, the experiments validate the two series of chilled water side control strategy. Every condition is repeated for three times to ensure the accuracy of the experimental results. And before the implement of every control strategy, the air conditioning system has to be kept continuous stable operation more than 0.5 h. The specific information of different conditions is summarized as shown in Table 4 in detail.

Table 1
List of sensors.

Sensor	Significance	Measurement precision
S1-T	outlet (i.e. supply) temperature of the chiller AND inlet temperature of the chilled water supply pipe	$\pm 0.1^\circ\text{C}$
S2-M	flow rate of the chilled water	$\pm 1\text{L/h}$
S3-T	inlet temperature of the cooling coil AND outlet temperature of the chilled water supply pipe	$\pm 0.1^\circ\text{C}$
S4-T	outlet temperature of the cooling coil AND inlet temperature of the chilled water return pipe	$\pm 0.1^\circ\text{C}$
S5-T	inlet (i.e. return) temperature of the chiller AND outlet temperature of the chilled water return pipe	$\pm 1^\circ\text{C}$
S6-TH	indoor air temperature and relative humidity, i.e. status of the return air	$\pm 0.01^\circ\text{C}$, $\pm 0.01\%$
S7-M	flow rate of the air	$\pm 10\text{m}^3/\text{h}$
S8-T	temperature of the supply air	$\pm 0.1^\circ\text{C}$

Table 2
Detailed information of the chiller, pipe and cooling coil.

Chiller	Model validation sensors: S1-T, S2-M and S5-T
Refrigerant type	R22
Rated cooling capacity	8.2 kW
Rated chilled water flow rate	1410 L/h
Mass of the evaporator	1.9 kg
Heat transfer area on the refrigerant side	2.86 m ²
Heat transfer area on the chilled water side	1.83 m ²
Chilled water mass in the evaporator	0.9 kg
Refrigerant mass in the evaporator	0.6 kg
Pipe	Model validation sensors: S1-T, S2-M and S3-T OR S2-M, S4-T and S5-T
Nominal diameter (Length)	DN40 (10m)
Nominal diameter (Length)	DN20 (1m)
Thickness of the insulation	40 mm
Cooling coil	Model validation sensors: S3-T, S4-T, S6-TH, S7-M and S8-T
Rated flow rate (maximum flow rate)	680 m ³ /h
Rated cooling capacity	3.74 kW

Table 3
Empirical constants in the thermal inertia model of the HVAC system.

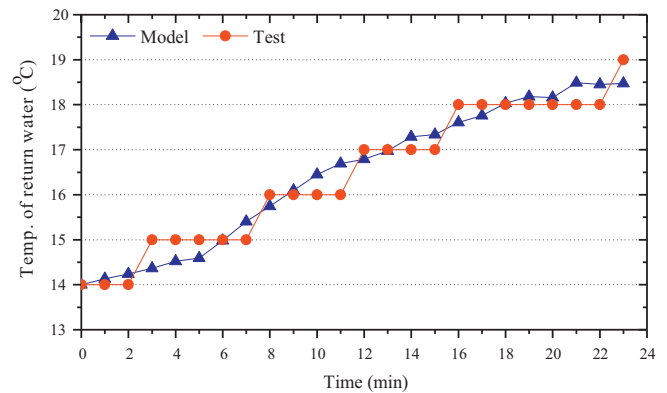
Constant	Value	Constant	Value	Constant	Value
C ₁	2896	C ₆	0.023	n ₄	0.85
C ₂	3942	C ₇	0.1	n ₅	n ₄
C ₃	8.6	n ₁	-0.2	n ₆	0.8
C ₄	4.2	n ₂	0.2	n ₇	0.3
C ₅	C ₄	n ₃	0.90	n ₈	0.33

4.2.2. Refrigerant cooling capacity

In the experiments, two series of DR control strategies were implemented in this system to validate the accuracy of the thermal inertia model of the chilled-water side: shut down the chiller and increase the setpoint of the return chilled-water temperature. Both DR control strategies were divided into two groups: one group

Table 4
Detailed information of the control strategies.

Control strategy	Description	Experimental condition
On/Off control	Shutting down the chiller (maintaining the chilled water pump operation)	The return chilled water temperature is stable at 14 °C, then shut down the chiller
Temperature increase	Temperature reset of the return chilled water	The return chilled water temperature is stable at 12 °C, then shut down the chiller
		Resetting the return chilled water from 12 °C to 14 °C
		Resetting the return chilled water from 10 °C to 14 °C

**Fig. 6.** Validation results of shutting down the chiller while maintaining the pump operation.

was used to evaluate the pattern of $Q(t)$ under different strategies and the other was used to validate the results of $Q(t)$.

4.2.2.1. Shut down the chiller. In the experiments performed to evaluate this strategy, the chiller was turned off while the chilled-water pump and FCU continued working.

In practical buildings, this strategy is commonly used around the off work time when the number of occupants gradually decreases. It is an energy conservation control strategy because the cooling capacity of the chilled water and materials can maintain the indoor air temperature for a time period. When a DR event occurs, this strategy can decrease the peak electricity demand of air-conditioning systems and maintain the indoor air temperature in the comfort zone.

The cooling capacity that plants generate is zero after shutting down the chiller; hence, the refrigerant cooling capacity $Q(t)$ of the chilled model should be 0. Before time step 0, the chiller is in the steady state, and the operation parameters of this state are the initial parameters of the model. The operation parameters of time step 1 were obtained by discretizing and calculating the differential Eq. (1)–(3). Then, the operation parameters of time step 1 were used as inputs to obtain the result of time step 2, and so on.

The model results when $Q(t)$ is set to 0 are shown in Fig. 6. The temperature of the return water increases after shutting down the chiller. The model results are consistent with the experiment

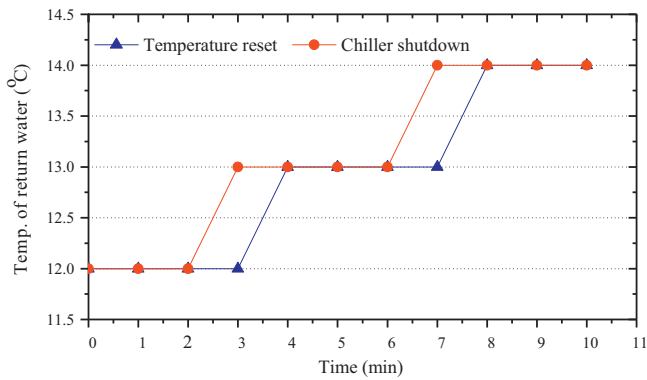


Fig. 7. Comparison of the experimental results of chilled-water temperature reset and chiller shutdown.

results, which indicates that the assumption that $Q(t)$ is 0 is reasonable and that the chiller model can be used to describe the temperature variation of the return water after shutting down the chiller.

The temperature of the return water is used as the model validation parameter because the chiller of the experiment platform can reset the return water temperature. It is helpful to obtain the variation pattern of $Q(t)$ for the temperature reset strategy by comparing the return water temperatures of these two strategies.

4.2.2.2. Reset temperature of the return chilled water. During the experiments used for this strategy, the setpoint of the return chilled water was increased. In the first group, the setpoint was reset from 12°C to 14°C.

Increasing the temperature setpoint of chilled water is another common DR strategy of the chiller side [8]. The cooling water system of this platform can only increase the temperature setpoint of the return water. The thermal inertia model of the chiller was used to describe the dynamic variation of the chilled-water temperature after the DR strategy was implemented, until a new steady state was reached. $Q(t)$ is unknown in the dynamic Eq. (1)–(3).

The unknown parameter in the model is commonly obtained by using the experiment results as the input parameter and the reverse calculation of the model. However, the experiments of return water temperature reset find that the increased velocity of the return water temperature for this strategy is more similar to the increased velocity of shutting down the chiller, which is shown in Fig. 7. Before time step 0, the chiller operates at a return water temperature of 12°C. At time step 0, the return water temperature is reset to 14°C. The experimental results of shutting down the chiller, as shown in Fig. 7, are identical to those shown in Figure. Before a new steady state is reached, the $Q(t)$ of the dynamic process is assumed to be 0 to increase the temperature setpoint of chilled water because this strategy appears similar to shutting down the chiller.

The calculation results of the model in Fig. 8 are consistent with the experimental results. Therefore, it is reasonable to assume that $Q(t)$ is 0 during a dynamic process.

4.2.3. Thermal inertia model validation

4.2.3.1. Validation of the single model. The dynamic models of the chiller, pipe and coil in this study can be validated by the experiments on the platform. The sensors used to validate each device are shown in Table 2. Two control strategies were conducted to validate the model: shutting down the chiller and resetting the return water temperature from 10 to 14°C.

4.2.3.1.1. Chiller model. The validation results of the chiller model are shown in Fig. 9(a), (b). The results verify the accuracy of Eq. (1)–(3) and the cooling capacity variations $Q(t)$ in section 4.1.2.

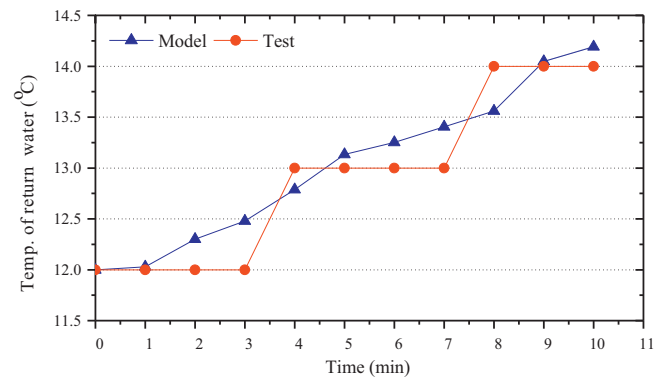


Fig. 8. Validation results of increasing the temperature setpoint of the return water.

The inputs of the chiller model are the initial operation parameters of the chiller, supply temperature and chilled-water flow rate at each time step (60 s), which were obtained from S1-T and S2-M. The temperatures of return water (S3-T) were used to validate the accuracy of the model.

The variation trend of return water temperatures of the chiller model is consistent with the trend of the test results. To assess the effectiveness of the model, the calculated results of the model were evaluated using the root mean square error (RMS), which is defined in Eq. (26) [46].

$$RMS = \sqrt{\frac{\sum_{i=1}^n (T_{model,i} - T_{test,i})^2}{n}} \quad (26)$$

The RMS of return chilled water temperature between chiller model prediction and experimental results under the two control strategies are 0.49°C and 0.43°C (Fig. 9(a), (b)) respectively, which indicates that the assumptions of the chiller model are reasonable, the thermal inertia model is accurate to some degree, and the cooling capacity variation $Q(t)$ in this paper is reasonable.

4.2.3.1.2. Coil model. The validation results of the cooling-coil model are shown in Fig. 9(c), (d), which demonstrates the accuracy of the thermal inertia Eq. (8)–(10) under dynamic conditions. The operation parameters of the steady state were used as the initial conditions. During the model computational process, the inputs of the coil model are the inlet temperature, flow rate of water, temperature, relative humidity and flow rate of return air per time step (60 s), which were obtained from S3-T, S2-M, S6-TH and S7-M. The state parameters of indoor air were used as the parameters of the return air. The temperatures of the supply air (S8-T) were used to validate the accuracy of the coil model.

The supply air temperatures calculated by the coil model are consistent with the test results except for some points. The RMS of return chilled water temperature between coil model prediction and experimental results under the two control strategies are 0.31°C and 0.28°C (Fig. 9(c), (d)) respectively, which indicates that the model in this paper is applicable to describe the thermal inertia of the coil.

4.2.3.1.3. Pipe model. The validation results of the pipe model are shown in Fig. 9(e), (f), which verifies the accuracy of the thermal inertia Eq. (20)–(21) under dynamic conditions. The initial conditions are the operation parameters of the steady state. During the computational process of the pipe model, the inputs of the pipe model are the inlet temperature of water obtained by S1-T per time step (60 s). The outlet temperatures of water were used to validate the accuracy of the pipe model.

The outlet water temperatures obtained by the pipe model are consistent with the test results. The RMS of return chilled water temperature between pipe model prediction and experimental

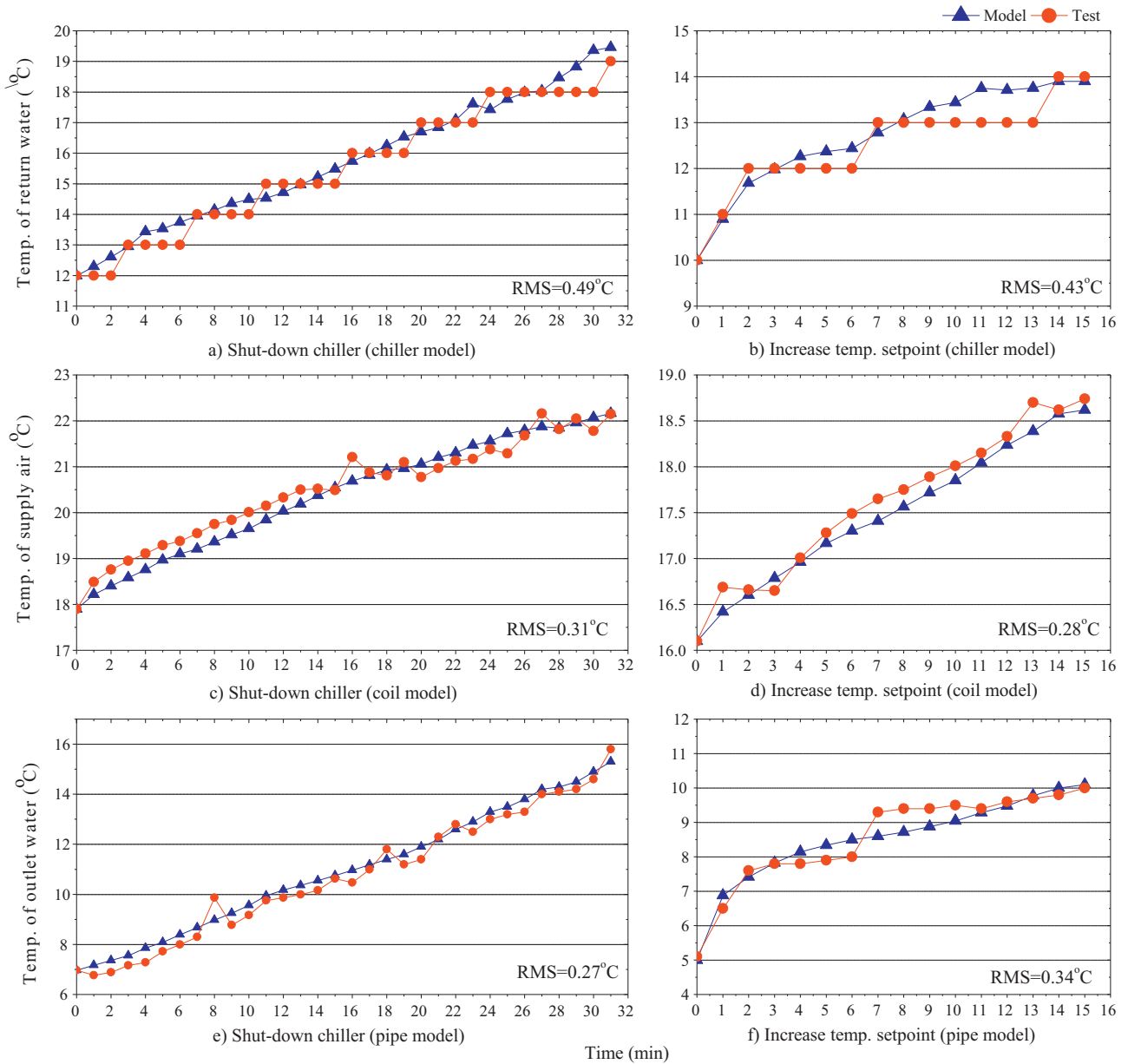


Fig. 9. Validation results of single models.

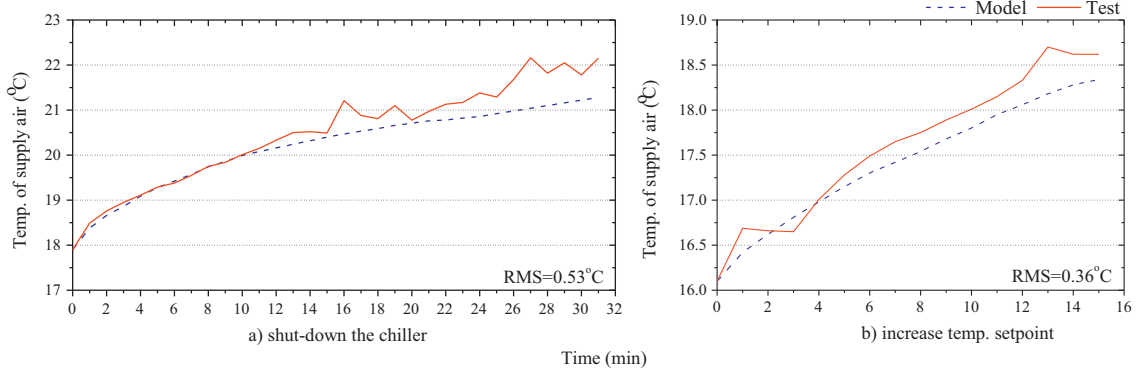


Fig. 10. Validation results of the entire model.

Table 5
Detailed information of the commercial chiller.

Description	Value	Description	Value
Rated chilled water flow rate	603m ³ /h	Mass of the evaporator	800 kg
Heat transfer area on the refrigerant side	765m ²	Heat transfer area on the chilled water side	545m ²
Chilled water mass in the evaporator	350 kg	Refrigerant mass in the evaporator	240 kg
C ₁	3132	n ₁	1.8
C ₂	4028	n ₂	-1.8

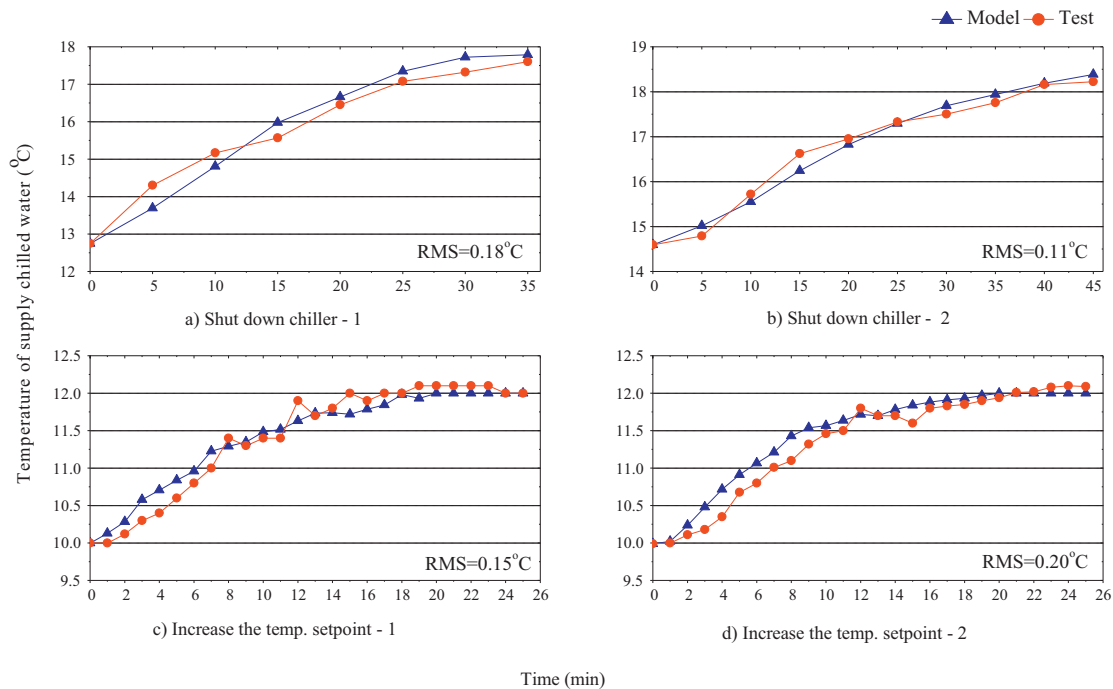


Fig. 11. Validation results of the commercial chiller.

results under the two control strategies are 0.27 °C and 0.34 °C (Fig. 9(e) (f)) respectively, which indicate that the thermal inertia model of pipes in this study is reasonably accurate.

4.2.3.2. Validation of the entire model. To apply the models in actual DR events, the accuracy of the entire system model is pivotal for the results. To validate the single model, the inputs of the models are the experimental values of each time step. When three models are combined as a single model, a complete loop is built, as shown in Figure. The input parameter of a model is the output parameter of the former model. For example, for the supply pipe, during the dynamic process after the DR strategy is implemented, the inlet water temperature of the pipe is the outlet water temperature of the chiller and the outlet water temperature of the pipe is the inlet temperature of the cooling coil. During the model validation, the initial conditions are the steady operation parameters before the DR strategy is implemented. During all experiments, the flow rate of chilled water was not adjusted, so the flow rate of chilled water is approximately a constant.

The purpose of the dynamic model in this study is to accurately describe the thermal inertia of the chilled water in DR events, i.e., to accurately estimate the cooling capacity supplied to terminals. In the experimental platform, the supply air temperature represents the cooling capacity because the flow is constant. Thus, the supply air temperature was selected as the parameter to evaluate the accuracy of the entire model.

The model was validated with two DR control strategies: shutting down the chiller and increasing the temperature setpoint of the returned chilled water. The results of the model coincide with the

experimental results well except several points, as shown in Fig. 10. The RMSs are 0.53 °C and 0.36 °C for the two control strategies.

4.3. Field validation of the chiller model

One chiller in a commercial building was used to further validate the thermal inertia model of the chillers and the patterns of $Q(t)$ under different DR control strategies of the plant side because the chiller model was simplified and $Q(t)$ is a newly introduced parameter in this study.

The operation parameters of the commercial chiller can be monitored and controlled by the control system, which can reset the temperature of the supply chilled water. The detailed information of the chiller is introduced in Table 5. Two series of experiments were conducted on the chiller: shutting down the chilled-water pump operation; increasing the setpoint of the supply chilled-water temperature. When the second strategy was implemented, the temperature setpoint of the supply chilled water was reset from 10 °C to 12 °C. Eq. (1)–(3) of the chiller thermal inertia model were validated by comparing the modeling and experimental results (Fig. 11).

The results of the model coincide with the experimental results, which indicate that:

- The simplified model of chillers in this study is reasonable;
- The recommended $Q(t)$ in the paper for the two types of DR strategies is generalized.

5. Conclusions and discussions

A dynamic model of chilled water systems in commercial buildings was developed in this paper to describe the thermal inertia of air-conditioning systems. Three individual sub-level models were developed: the chiller model, cooling-coil model and pipe model. The purpose of the model is to describe the variation of supply cooling capacity to zones after DR strategies are implemented. The refrigerant cooling capacity $Q(t)$ was introduced in this study to simplify the chiller model. The variation patterns of $Q(t)$ for two types of DR strategies (shutting down the chiller and increasing the temperature setpoint of chilled water) were obtained and experimentally validated. The sub-level models and the entire model were experimentally validated.

The conclusions of this study are as follows:

- The refrigerant cooling capacity $Q(t)$ is equal to 0 for the dynamic processes after shutting down the chiller and increasing the temperature setpoint of the chilled water; $Q(t)$ is calculated based on the temperature difference between the supply and return water and the flow rate of chilled water during the steady state;
- The sub-level models are reasonably accurate. The results of the chiller model, cooling-coil model and pipe model coincide with the experimental results;
- The calculated variation tendency of the supply air temperatures using the entire thermal inertia model is similar to the tendency of the experimental results. The RMS is 0.43 °C and 0.16 °C for the two control strategies.

The chiller model and value of the refrigerant cooling capacity $Q(t)$ are further validated by a commercial chiller in a building.

In summary, the thermal inertia model of the chilled water systems in this paper can accurately describe the dynamic heat transfer of chilled water side. In the DR-related study, the model can combine with the thermal inertia model of buildings to evaluate the variation of zone temperatures during DR.

The thermal inertia model of a chilled-water system in this paper aims to accurately describe the dynamic variation of the cooling capacity that is supplied to the zones after DR strategies are implemented. However, because of the limitation of the experimental conditions, the study only verified the model for two common DR strategies. Thus, the applicability of the model for other DR control strategies requires further validation. More experiments will be conducted to test other control strategies in the future.

Acknowledgment

This research was funded by the technology and science project of the State Grid Corporation of China (No. SGZJ000BGJS1500460).

References

- [1] L. Pérez-Lombard, J. Ortiz, C. Pout, A review on buildings energy consumption information[J], *Energy Build.* 40 (3) (2008) 394–398.
- [2] J. Virote, N.S. Rui, Stochastic models for building energy prediction based on occupant behavior assessment, *Energy Build.* 53 (10) (2012) 183–193.
- [3] M. Fasiuddin, I. Budaiwi, HVAC system strategies for energy conservation in commercial buildings in Saudi Arabia, *Energy Build.* 43 (12) (2011) 3457–3466.
- [4] T.N.T. Lam, K.K.W. Wan, S.L. Wong, et al., Impact of climate change on commercial sector air conditioning energy consumption in subtropical Hong Kong, *Appl. Energy* 87 (7) (2010) 2321–2327.
- [5] G.S. Pavlak, G.P. Henze, V.J. Cushing, Optimizing commercial building participation in energy and ancillary service markets, *Energy Build.* 81 (2014) 115–126.
- [6] R. Yin, P. Xu, M.A. Piette, et al., Study on Auto-DR and pre-cooling of commercial buildings with thermal mass in California, *Energy Build.* 42 (7) (2010) 967–975.
- [7] Y.C. Li, S.H. Hong, BACnet?EnOcean Smart Grid Gateway and its application to demand response in buildings, *Energy Build.* 78 (4) (2014) 183–191.
- [8] M.H. Albadi, E.F. El-Saadany, Demand Res. Electricity Markets: Overview 14 (9) (2007) 1–5.
- [9] N. Motegi, M.A. Piette, D.S. Watson, S. Kilicott, P. Xu, Introduction to commercial building control strategies and techniques for demand response, *Build. Energy Simul. User News* 2007 (11) (2007) A1–A19.
- [10] T.M. Braun, C.J. Klaass, J.M. House, Demonstration of load shifting and peak load reduction with control of building thermal mass, in: *Proceedings of the 2002 ACEEE Conference on Energy Efficiency in Buildings*, Monterey, CA (2002), 2002.
- [11] James E. Braun, K.H. Lee, An experimental evaluation of demand limiting using building thermal mass in a small commercial building, *Ashrae Trans.* 112 (2006) 559–571.
- [12] P. Xu, P. Haves, Case study of demand shifting with thermal mass in two large commercial buildings, *Ashrae Trans.* 112 (3) (2006) 572–580.
- [13] P. Xu, P. Haves, M.A. Piette, et al., Peak demand reduction from pre-cooling with zone temperature reset in an office building, *Lawrence Berkeley National Laboratory* 14 (2) (2006), 83–89(7).
- [14] K.-H. Lee, J.E. Braun, A data-driven method for determining zone temperature trajectories that minimize peak electrical demand, *ASHRAE Transactions* 114 (2) (2008), 65(10).
- [15] J.E. Lee K.-h. Braun, Development of methods for determining demand-limiting setpoint trajectories in buildings using short-term measurements, *Build. Environ.* 43 (10) (2008) 1755–1768.
- [16] K.-H. Lee, J.E. Braun, Evaluation of methods for determining demand-limiting setpoint trajectories in buildings using short-term measurements, *Build. Environ.* 43 (10) (2008) 1769–1783.
- [17] X. Li, A. Malkawi, Multi-objective optimization for thermal mass model predictive control in small and medium size commercial buildings under summer weather conditions, *Energy* 112 (2016) 1194–1206.
- [18] R. Yin, E.C. Kara, Y. Li, et al., Quantifying flexibility of commercial and residential loads for demand response using setpoint changes, *Appl. Energy* 177 (2016) 149–164.
- [19] X. Xue, S. Wang, C. Yan, et al., A fast chiller power demand response control strategy for buildings connected to smart grid, *Appl. Energy* 137 (2015) 77–87.
- [20] Keeney, R. Kevin, J.E. Braun, D. Ph, Application of building precooling to reduce peak cooling requirements, *Ashrae Trans.* (1997) 463–469.
- [21] Hongkun Song, Yang Li, Guoqing Tang Research on duty cycling control for central air conditioning system, *Electric Power* 36 (3) (2003) 35–38.
- [22] W. Li, P. Xu, H. Wang, et al., A new method for calculating the thermal effects of irregular internal mass in buildings under demand response, *Energy Build.* (130) (2016) 761–772.
- [23] S. Bendapudi, J.E. Braun, E.A. Groll, A comparison of moving-boundary and finite-volume formulations for transients in centrifugal chillers, *Int. J. Refrig.* 31 (8) (2008) 1437–1452.
- [24] Pengfei Li, Hongtao Qiao, Yaoyu Li, et al., Recent advances in dynamic modeling of HVAC equipment. part 1: equipment modeling, *Hvac & R Research* 20 (1) (2014) 136–149.
- [25] Pengfei Li, Yaoyu Li, E. John Seem, et al., Recent advances in dynamic modeling of HVAC equipment. Part 2: Modelica-based modeling, *Hvac & R Research* 20 (1) (2014) 150–161.
- [26] S. Wang, Dynamic simulation of building VAV air-conditioning system and evaluation of EMCS on-line control strategies, *Build. Environ.* 34 (6) (1999) 681–705.
- [27] C. Wu, Z. Xingxi, D. Shiming, Development of control method and dynamic model for multi-evaporator air conditioners (MEAC), *Energy Convers. Manage.* 46 (3) (2005) 451–465.
- [28] B. Tashtoush, M. Molhim, M. Al-Rousan, Dynamic model of an HVAC system for control analysis, *Energy* 30 (10) (2005) 1729–1745.
- [29] M. Mossolly, K. Ghali, N. Ghaddar, Optimal control strategy for a multi-zone air conditioning system using a genetic algorithm, *Energy* 34 (1) (2009) 58–66.
- [30] G. Platt, J. Li, R. Li, et al., Adaptive HVAC zone modeling for sustainable buildings, *Energy Build.* 42 (4) (2010) 412–421.
- [31] P. Schalbart, P. Haberschild, Simulation of the behavior of a centrifugal chiller during quick start-up, *Int. J. Refrig.* 36 (1) (2013) 222–236.
- [32] H. Bechtler, M.W. Browne, P.K. Bansal, et al., New approach to dynamic modelling of vapour-compression liquid chillers: artificial neural networks, *Appl. Therm. Eng.* 21 (9) (2001) 941–953.
- [33] M. Hosoz, H.M. Ertunc, Modelling of a cascade refrigeration system using artificial neural network, *Int. J. Energy Res.* 30 (14) (2006) 1200–1215.
- [34] B.P. Rasmussen, A.G. Alleyne, R], in: *Dynamic Modeling and Advanced Control of Air Conditioning and Refrigeration Systems*, Air Conditioning and Refrigeration Center. College of Engineering. University of Illinois at Urbana-Champaign., 2006, 2017.
- [35] X. Li, W. Jin, E.W. Bai, Developing a whole building cooling energy forecasting model for on-line operation optimization using proactive system identification, *Appl. Energy* 164 (164) (2016) 69–88.
- [36] Y. Yao, M. Huang, J. Chen, State-space model for dynamic behavior of vapor compression liquid chiller, *Int. J. Refrig.* 36 (8) (2013) 2128–2147.
- [37] G.L. Wedekind, B.L. Bhatt, B.T. Beck, A system mean void fraction model for predicting various transient phenomena associated with two phase evaporating and condensing flows, *Int. J. Multiphase Flow* 4 (1978) 97–114.
- [38] D. Shiming, A dynamic mathematical model of a direct expansion (DX) water-cooled air-conditioning plant, *Build. Environ.* 35 (7) (2000) 603–613.
- [39] B.P. Rasmussen, R. Shah, A.B. et al. Musser, Control-oriented Modeling of Transcritical Vapor Compression Systems, *Air Conditioning and Refrigeration*

- Center. College of Engineering. University of Illinois at Urbana-Champaign, 2002.
- [40] M.W. Browne, P.K. Bansal, Transient simulation of vapour-compression packaged liquid chillers, *Int. J. Refrig.* 25 (5) (2002) 597–610.
- [41] L. Zhao, M. Zaheeruddin, Dynamic simulation and analysis of a water chiller refrigeration system, *Appl. Therm. Eng.* 25 (14–15) (2005) 2258–2271.
- [42] R. Llopis, R. Cabello, E. Torrella, A dynamic model of a shell-and-tube condenser operating in a vapour compression refrigeration plant, *Int. J. Therm. Sci.* 47 (7) (2008) 926–934.
- [43] T.K. Nunes, J.V.C. Vargas, J.C. Ordóñez, et al., Modeling, simulation and optimization of a vapor compression refrigeration system dynamic and steady state response, *Appl. Energy*. 158 (2015) 540–555.
- [44] X. Yu, J. Wen, T.F. Smith, A model for the dynamic response of a cooling coil, *Energy Build.* 37 (12) (2005) 1278–1289.
- [45] C.K. Lee, A simplified explicit model for determining the performance of a chilled water cooling coil, *Int. J. Refrig.* 43 (7) (2014) 167–175.
- [46] G.Y. Jin, W.J. Cai, Y.W. Wang, et al., A simple dynamic model of cooling coil unit, *Energy Convers. Manage.* 47 (15–16) (2006) 2659–2672.
- [47] Xiaotang Zhou, E. James, Braun a simplified dynamic model for chilled-Water cooling and dehumidifying Coils—Part 1: development (RP-1194), *Hvac & R Res.* 13 (5) (2007) 785–804.
- [48] Xiaotang Zhou, E. James, Braun a simplified dynamic model for chilled-Water cooling and dehumidifying Coils—Part 2: experimental validation (RP1194), *Hvac & R Res.* 13 (5) (2007) 805–817.
- [49] X. Zhou, Dynamic Modeling of Chilled Water Cooling Coils, Purdue University., 2005.
- [50] EnergyPlus, EnergyPlus Engineering Reference, Lawrence Berkeley National Laboratory, 2009.
- [51] TRNSYS, A Transient Simulation Program, Solar energy laboratory, University of Wisconsin, Madison, WI, U.S.A, 1990.
- [52] V.I. Hanby, J.A. Wright, D.W. Fletcher, et al., Modeling the dynamic response of conduits, *Hvac & R Res.* 8 (1) (2002) 1–12.
- [53] N. Liang, S. Shao, C. Tian, et al., Dynamic simulation of variable capacity refrigeration systems under abnormal conditions, *Appl. Therm. Eng.* 30 (10) (2010) 1205–1214.
- [54] X.M. Zhang, Z.P. Ren, F.M. Mei, Heat transfer theory (the fifth edition) [M] 153–154, Chin. Archit. Building Press (2007) 153–154 (and 170).